

Observation of Optical Solitons and Abnormal Modulation Instability in Liquid Crystals with Negative Dielectric Anisotropy

Jing Wang¹, Zhenlei Ma¹, Junzhu Chen¹, Jinlong Liu^{1,2}, Zhuo Wang¹, Yiheng Li¹, Qi Guo^{1,4}, Wei Hu^{1,5}, and Li Xuan³

¹Guangdong Province Key Laboratory of Nanophotonic Functional Materials and Devices,
South China Normal University, Guangzhou 510006, China

²College of Science, South China Agricultural University, Guangzhou, 510642, China

³State Key Laboratory of Applied Optics, Changchun Institute of Optics,
Fine Mechanics and Physics, Chinese Academy of Sciences, Changchun 130033, China

⁴Corresponding author: guoq@scnu.edu.cn and

⁵Corresponding author: huwei@scnu.edu.cn

(Dated: March 9, 2015)

We investigate theoretically and experimentally the optical beam propagation in the nematic liquid crystal with negative dielectric anisotropy, which is aligned homeotropically in a $80\mu\text{m}$ -thickness planar cell in the presence of an externally voltage. It is predicted that the nonlocal nonlinearity of liquid crystal undergo an oscillatory response function with a negative nonlinear refractive index coefficient. We found that the oscillatory nonlocal nonlinearity can support stable bright solitons, which are observed in experiment. We also found that abnormal modulation instability occurs with infinity gain coefficient at a fixed spatial frequency, which is no depend on the beam intensity. We observed the modulation instability in the liquid crystal at a very low intensity ($0.26\text{W}/\text{cm}^2$), and the maximum gain frequency were found kept unchange when beam power changes over 2-3 orders of magnitude.

I. INTRODUCTION

Nonlocal solitons, solitons in nonlinear media with a nonlocal response, have been the subject of intense theoretical and experimental studies in many physical systems [1, 2], including photorefractive crystals [3], nematic liquid crystals [4–7], lead glasses [8, 9], liquids [10, 11], liquid-filled photonic crystal fibers [12, 13], atomic vapors [14], and Bose-Einstein condensates [15, 16]. There are various types of nonlocal solitons, such as vortex solitons [17, 18], multipole solitons [19, 20], and soliton clusters [21–24]. Nonlocal solitons have a number of interesting properties, including large phase shift [25], attraction between two out-of-phase solitons [7, 10], a self-induced fractional Fourier transform [26], and suppression of the collapse instability [27].

In the nonlocal response in nonlinear media, the refractive index change at a given point is determined not only by the light intensity at that point but also by the light intensity near that point, which can be described by a nonlocal response function. There are several types of nonlocal response in real nonlinear media, such as the zeroth-order modified Bessel nonlocal response in nematic liquid crystals [7], the logarithmic nonlocal response in lead glass [28], and the exponential-decay type nonlocal response in aqueous solution of rhodamine B [29] and diluted India ink [30]. All these response functions are integrable functions with non-negative value.

Nikolov *et al.* found that quadratic solitons are equivalent to nonlocal solitons on the basis of an analogy between parametric interaction and diffusive nonlocality [31]. The nonlocal analogy was later used to successfully describe pulse compression [32, 33], localized X waves [34], and modulational instability [35] in $\chi^{(2)}$ materials. Nikolov *et al.* showed that the second har-

monic (SH), like the nonlinear refractive index forming a waveguide, traps the fundamental wave (FW). They found two types of response functions, the exponential-decay type and the sine-oscillatory type. On the basis of the sine-oscillatory type response function, one can understand why Buryak and Kivshar found numerically that quadratic solitons radiate linear waves [31, 36]. In 2012, Esbensen *et al.* further investigated quadratic solitons with a sine-oscillatory type response function and found a family of analytical solutions under the strongly nonlocal approximation [37]. However, these soliton solutions, whether numerical or analytical, were all unstable. We have shown that boundary conditions can stabilize this type of nonlocal soliton with sine-oscillatory response functions [38]. In this letter, we will demonstrate that nematic liquid crystal with negative dielectric anisotropy is new media which has oscillatory response functions.

Nematicons, spatial optical solitons in nematic liquid crystals (NLC), have been the subject of intense theoretical and experimental studies over the past two decades [39]. The pioneering work on nematicons was reported in 1993 by Braun *et al.* [40]. They investigated the strong self-focusing of a laser beam in NLC in various geometries, from which they recognized the importance of molecular reorientation and anchoring at the boundaries. Subsequently, in 1998, Warengem *et al.* observed the beam self-trapping in capillaries filled with dye-doped NLC [41]. In the same year, Karpierz *et al.* observed the same phenomenon in planar cells with homeotropically aligned NLC [42]. They lowered the required power of observing nematicons to milliwatt levels. In 2000, Pecianti *et al.* reported on nematicon formation in planar cells containing a NLC aligned homogeneously in the presence of an externally applied voltage [43]. They extended the propagation length of nematicons for millime-

ter levels and found the adequate model for describing nematicon propagation.

The investigation on nematicon was sparse until Conti *et al.* found that the NLC with a pretilt angle induced by an external low-frequency electric field is a kind of strongly nonlocal nonlinear medium and nematicons are a kind of accessible solitons [1, 4, 5]. They derived a simplified model and linked nematicons with quadratic solitons. The basic properties on nematicon have been revealed gradually ever since. Among others, we have to mention the interactions between two nematicons [7, 44–46]. Recently, Piccardi *et al.* reported the dark nematicon formation in planar cells filled with dye-doped NLC aligned homeotropically, which can provide an effective negative nonlinearity [47]. The negative nonlinearity is realized through the guest-host interaction.

In this letter, we observed the nematicon formation in planar cells containing a NLC with negative dielectric anisotropy and positive optical anisotropy homeotropically aligned in the presence of an externally applied voltage. Following the method in [4], we got a simplified model with a negative Kerr coefficient and an oscillatory periodic response function, which can support bright nematicons. We outlined the connection between the simplified model and the equations describing quadratic solitons [31, 36–38].

II. PHYSICAL MODEL AND SOLITON

We performed a series of experiments to observe the nematicon formation in NLC with negative dielectric anisotropy. The experimental setup is illustrated in Fig. 1(a). A light beam from a Verdi laser was focused by a 10X microscope objective and launched into a 80- μm -thick NLC cell. The configuration of the cell was shown in Fig. 1(b) and the cell was filled with the homeotropically aligned KY19-008 NLC, whose $n_{\parallel} = 1.726$, $n_{\perp} = 1.496$, average elastic constant $K = 1 \times 10^{-11}\text{N}$, optical anisotropy $\epsilon_a^{op} = 0.74106$, and dielectric anisotropy $\epsilon_a^{rf} = -5.3$. Owing to the negative dielectric anisotropy, the NLC molecules will try to adjust in a low-frequency applied electrical field in such a manner that the molecule axes turn perpendicular to the direction of the electric field [48]. A microscope and a CCD camera were used to collect the light scattered above the cell during propagation.

In the presence of an externally applied (low-frequency) electric field E_{rf} , the evolution of the slowly varying envelope A of a paraxial optical beam linearly polarized along X (an extraordinary light) and propagating along Z can be described by the system,

$$2ik \frac{\partial A}{\partial Z} + \nabla_{XY}^2 A + k_0^2 \epsilon_a^{op} (\sin^2 \theta - \sin^2 \theta_0) A = 0, \quad (1)$$

$$2K \left(\frac{\partial^2 \theta}{\partial Z^2} + \nabla_{XY}^2 \theta \right) + \epsilon_0 (\epsilon_a^{rf} E_{rf}^2 + \epsilon_a^{op} \frac{|A|^2}{2}) \sin(2\theta) = 0, \quad (2)$$

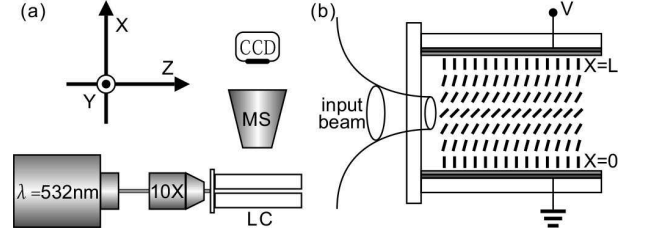


FIG. 1. Sketch of the experimental setup (a) and homeotropically aligned nematic liquid crystal cell (b) for the observation of nematicons.

where ϵ_0 is the vacuum permittivity, θ is the tilt angle of the NLC molecules, θ_0 is the nadir tilt in the absence of light, $k = k_0 n_e(\theta_0)$ with k_0 the vacuum wavenumber and $n_e(\theta_0) = n_{\perp} n_{\parallel} / (n_{\parallel}^2 \cos^2 \theta_0 + n_{\perp}^2 \sin^2 \theta_0)^{1/2} \approx (n_{\perp}^2 + \epsilon_a^{op} \sin^2 \theta_0)^{1/2}$ the refractive index of the extraordinary light at θ_0 , $\nabla_{XY}^2 = \partial_X^2 + \partial_Y^2$, $\epsilon_a^{rf} = \epsilon_{\parallel} - \epsilon_{\perp} (< 0)$, $\epsilon_a^{op} = n_{\parallel}^2 - n_{\perp}^2 (> 0)$. The term $\partial_Z^2 \theta$ in Eq.(2) was proven to be negligible compared to $\nabla_{XY}^2 \theta$, therefore it can be removed. The homeotropical boundaries and anchoring at the interfaces define $\theta|_{X=0} = \theta|_{X=L} = \pi/2$, where L is the cell thickness. In the absence of light, the pretilt angle $\hat{\theta}$ is symmetric along X about $X = L/2$ (the cell center) and depends only on X :

$$2K \frac{\partial^2 \hat{\theta}}{\partial X^2} + \epsilon_0 \epsilon_a^{rf} E_{rf}^2 \sin(2\hat{\theta}) = 0. \quad (3)$$

As the external bias voltage increasing, the nadir tilt angle θ_0 decreases when the voltage is above the Fréedericks threshold.

Furthermore, analogous to the theory for nematicon in positive NLC[6], we can set $\theta = \hat{\theta} + (\hat{\theta}/\theta_0)\Phi$, with Φ being the optically induced perturbation. Noting that $\hat{\theta} \approx \theta_0$ and $\partial_X \hat{\theta} \approx 0$ in the middle of the cell when the beam width w_0 is far smaller than the cell thickness, we can simplify Eq.(1) and Eq.(2) into the following system, which describes the coupling between A and Φ :

$$2ik \frac{\partial A}{\partial Z} + \nabla_{XY}^2 A + 2n_0 k_0^2 \Delta n A = 0, \quad (4)$$

$$w_m^2 \nabla_{XY}^2 \Delta n + \Delta n = n_2 |A|^2, \quad (5)$$

where the nonlinear changes of diffraction index $\Delta n = \epsilon_a^{op} \sin(2\theta_0)\Phi/2n_0$, the parameter w_m ($w_m > 0$ for $|\theta_0| \leq \pi/2$) is the characteristic length of the nonlinear response function, reads:

$$w_m = \frac{1}{E_{rf}} \left\{ \frac{2\theta_0 K}{\epsilon_0 |\epsilon_a^{rf}| \sin(2\theta_0) [1 - 2\theta_0 \cot(2\theta_0)]} \right\}^{1/2}, \quad (6)$$

and

$$n_2 = - \frac{(\epsilon_a^{op})^2 \theta_0 \sin(2\theta_0)}{4n_0 |\epsilon_a^{rf}| E_{rf}^2 [1 - 2\theta_0 \cot(2\theta_0)]}. \quad (7)$$

The nonlinear refractive index coefficient n_2 is defined as suggested by Peccianti et al.[6].

The nonlocal nonlinearity in negative NLC described by Eq. (5) is extraordinary than common nonlocal nonlinearity. First, the nonlinear refractive index coefficient n_2 is negative for negative NLC, while it is positive for positive NLC. Secondly and more importantly, the response function described by Eq. (5) is oscillatory, given as (in 1+2D)

$$R(r) = Y_0(r/w_m)/(4w_m^2), \quad (8)$$

or $R(x) = \sin(x/w_m)/(2w_m)$ (in 1+1D), where $r^2 = x^2 + y^2$, $Y_0(\cdot)$ is zero-order Bessel function of the second kind. Then the nonlinear change of diffraction index Δn is given as

$$\Delta n(r) = n_2 \int_{-\infty}^{\infty} R(r-r')|A(r')|^2 d^D r', \quad (9)$$

where $\vec{r} = x\vec{i} + y\vec{j}$ for 1+2D(D=2) or $r = x$ for 1+1D(D=1). The response functions for negative NLC are not integrable, and it can not be normalized using the condition $\int_{-\infty}^{\infty} R(r)dr = 1$. In local limit case (when w_m approach zero), we have $\Delta n = n_2|A|^2$ from Eq.(5) and nonlinearity is self-defocusing. But the response function Eq.(8) can not approach a delta function mathematically.

It is very interesting to investigate asymptotic behavior of these response functions for r approach zero. From Eq.(8), we have $R(r) \approx \ln(r/2w_m)/2\pi w_m^2$ for $r \rightarrow 0$, and it approach negative infinity. Considering that $n_2 < 0$ so the effective asymptotic function is $-\ln(r/2w_m)/2\pi w_m^2$, which is identical to the asymptotic function for positive NLC. For positive NLC, the response function is $R(r) = K_0(r/w_m)/(2\pi w_m^2)$, where $K_0(\cdot)$ is zero-order modified Bessel function of the second kind[6, 7]. The same asymptotic functions for positive and negative NLC imply that under the strongly nonlocal approximation ($w_m \gg w_0$), the nonlinearity in negative NLC is self-focusing, although the nonlinear refractive index coefficient n_2 is negative. That means we can observe the bright soliton in negative NLC. Our numerical simulation and experimental observation confirmed our prediction as shown in Fig.2.

Numerical simulation of beam propagation were carried out based on Eq.(1) and Eq.(2) with Gaussian beam as an incident profile. For low power input or without the bias voltage, no nonlinear effect occurs and beams undergo linear diffraction as shown in Fig.2(a). When increase beam power and bias voltage, we can found stable bright solitons as shown in Fig.2(b).

In experiment, the launched power and beam width are fixed to $P_0 = 4.42mW$ and $w_0 = 4\mu m$. For x -polarized beam (e -light), optically induced molecular reorientation occurs and contributes to the nonlinear index change. So soliton can be observed only for x -polarized beam. Fig. 2(c) shows the linear diffraction in absence of the bias and Fig. 2(d) shows the nematic soliton formation at $V =$

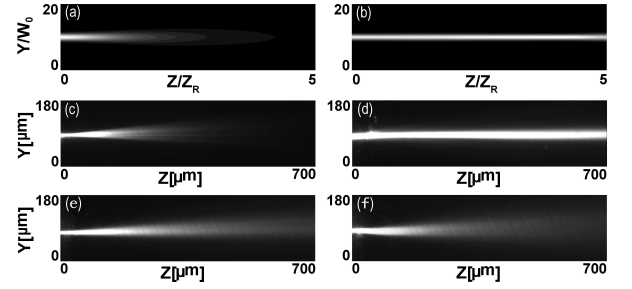


FIG. 2. (a)-(b) Numerical simulation of beam propagation based on Eq.(1) and Eq.(2) for (a) linear diffraction and (b) soliton propagation. (c)-(d) X -polarized e -beam propagation for (c) without voltage bias (linear diffraction) and (d) in the presence of 3.4 V at 1 kHz (soliton propagation). (e)-(f) Y -polarized o -beam propagation (linear diffraction) for (e) without voltage bias and (f) without voltage bias. Beam power $P = 4.42mW$ and beam width $w = 4\mu m$ in (c)-(f).

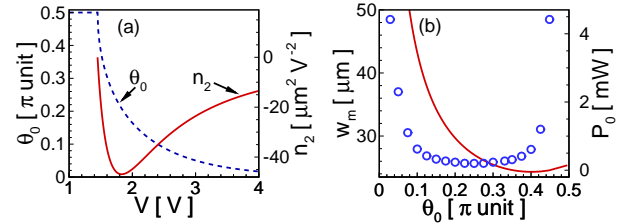


FIG. 3. (Color online) (a) The pretilt angle θ_0 and the Kerr coefficient n_2 of the NLC vs the bias voltage V . (b) The characteristic length w_m (a solid curve) and the critical power of a single soliton (circles) vs the pretilt angle θ_0 . The parameters are for a $80 - \mu m$ -thick cell filled with the NLC (KY19-008) and the critical power is a numerical result.

3.4V, which is above the Fréedericks threshold. For y -polarized beam (o -light), the nonlinearity does not occur and only diffraction beam can be observed, as shown in fig. 2(e) and 2(f).

The variations of characteristic length w_m and Kerr coefficient n_2 dependence on pretilt angle θ_0 and the bias voltage V are given in Fig.3. A monotonous function of θ_0 on E_{rf} (or V by $V = E_{rf}L$) is described by Eq. (3). As shown in Fig. 3(a), θ_0 decreases monotonously from $\pi/2$ to 0 with increasing the bias above the Fréedericks threshold. The Fréedericks threshold can be found [6, 49]

$$V_{fr} = \pi \left(\frac{K}{\epsilon_0 |\epsilon_a^{rf}|} \right)^{1/2}. \quad (10)$$

Introducing the value of ϵ_a^{rf} and K for KY19-008 NLC, we can get $V_{fr} \approx 1.45V$. For E_{rf} higher than the Fréedericksz threshold, the approximation

$$\theta_0 \approx \frac{\pi}{2} \left(\frac{E_{fr}}{E_{rf}} \right)^3 \quad (11)$$

is satisfactory, where $E_{fr} = V_{fr}/L$. Therefore, we can clearly see from Eqs.(6) and (7) that w_m and n_2 are determined by V or θ_0 for a given NLC cell configuration.

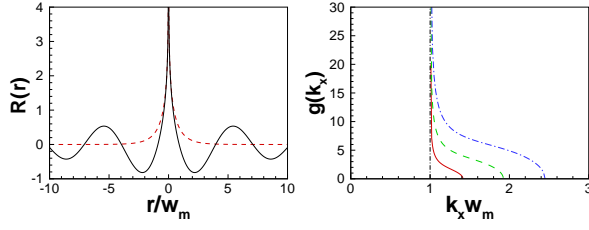


FIG. 4. (Color online) (a) (1+2)D response function for negative (solid) and positive (dashed) NLC. (b) The modulation Instability gain for different beam power, $2n_0 k_0^2 n_2 A_0^2 = 1, 5, 10$.

As shown in Fig. 3, w_m and n_2 changes nonmonotonously with increasing θ_0 and V , respectively. Both of them have a minimum value. There we also show the relation of the critical power P_0 on θ_0 calculating numerically based on Eqs. (1)–(2) with Gaussian beam as an incident profile.

III. MODULATION INSTABILITY

The oscillatory-type response functions are singularity in the frequency spectrum [38]. The response function $R(r)$ in the Fourier domain k_\perp is

$$\tilde{R}(k_\perp) = 1/(1 - w_m^2 k_\perp^2), \quad (12)$$

where k_\perp is transverse spatial frequency. It is singular when $k_\perp = 1/w_m$. This singularity induce an abnormal MI in negative NLC.

Using the standard process, from Eq. 4 and 5 we find the MI occurs in negative NLC when

$$k_c^2 < k_\perp^2 < \frac{k_c^2}{2} + \frac{k_c^2}{2} \sqrt{(1 + 16n_0 k_0^2 |n_2| A_0^2)}, \quad (13)$$

where $k_c = 1/w_m$ is the singular frequency, A_0 is the amplitude of background planar wave. The MI gain factor g is given as

$$g(k_\perp) = \frac{|k_\perp|}{n_0 k_0} \sqrt{\frac{(k_\perp^4 - k_c^2 k_\perp^2 + 4n_0 k_0^2 \gamma A_0^2 k_c^2)}{(k_c^2 - k_\perp^2)}}. \quad (14)$$

Figure 4(a) shows the profile of response functions for both negative and positive NLC. MI gain spectrum for different beam power was shown in Fig.4(b). We can see that at the singular frequency k_c , the MI gain factor is also singular and its value approaches infinity. When beam power increases, the MI range increases but the singular frequency keeps unchanged. We can predict that MI will occur at an extremely low power due to the infinity value of MI gain at the singular frequency k_c , which is independent on beam power.

We observed the abnormal MI in negative NLC using the same experimental configuration as Fig.1(a). The 10X-objective lens is replaced by a cylindrical lens with focal length 25mm to produce an ellipse beam with

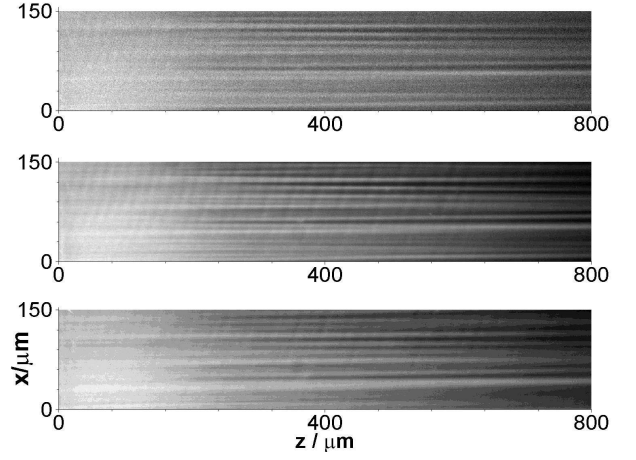


FIG. 5. Experimental observation of MI for different power, $P_0 = 0.06mW, 1.0mW, 100mW$, from top to bottom, respectively. The brightness of photo was increased for clear by software.

dimension of $10\mu m \times 2.3mm$. The ellipse beam was launched into the NLC cell and part of the beam was recorded by CCD, as shown in Fig.5. We have observed that MI occurs at low beam power of $0.06mW$, corresponding to beam intensity $0.26W/cm^2$. In our knowledge, it is the lowest intensity to induce MI in experiment.

We read the intensity profiles from these photos and calculate the spatial spectrum at different z -distance. By removing the initial spatial spectrum at $z = 0\mu m$, we get the relative MI gain spectrum for several distances. The maximum MI gain frequencies K_M are gotten and given in Fig.6(a). One can see that the maximum MI gain frequencies fluctuate around $K_M \approx 0.05\mu m^{-1}$ when beam power changes from $0.06mw$ to $170mW$, over 3-order of magnitude. From our theory ($k_c = 1/w_m$), $K_M \approx 0.05\mu m^{-1}$ means the nonlinear characteristic length $w_m \approx 20\mu m$, which is near the value gotten from Eq. (6). We also observed the maximum MI gain frequency for different bias voltage, as shown in Fig.6(a). At $z = 400\mu m$, K_M decreases as increasing voltage. So we get the characteristic length w_m decreases as increasing θ_0 , same as shown in Fig.3(b). However, the value of w_m gotten from K_M is always 3-4 times smaller than that in Fig.3(b).

IV. CONCLUSION

In summary, we observed experimentally the nematicon formation in the planar cell containing the nematic liquid crystal with negative dielectric anisotropy, aligned homeotropically in the presence of an externally applied voltage. We found that the nonlocal nonlinearity in this system undergoes an oscillatory response function with a negative nonlinear refractive index coefficient. The singularity of the oscillatory-type response functions induces

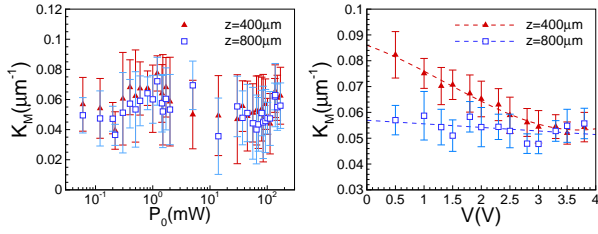


FIG. 6. (a) Maximum MI gain frequency varies on the beam power, bias voltage $V = 3.4V$. (b) Maximum MI gain frequency varies bias voltage.

an abnormal modulation instability, in which MI gain at singular frequency are infinity. In experiment, we have observed that MI occurs at an extremely low beam inten-

sity about $0.26W/cm^2$. So we demonstrate that negative NLC is new media with extraordinary oscillatory-type nonlocal nonlinearity.

The singularity of the oscillatory-type response function comes from the fact that the function extends to infinity in all space. If the oscillatory-type response function is limited within a finite space, the singularity will be suppressed [38]. If we consider the response delay time, the oscillatory-type response function will be localized in space by a finite time. In this letter, the response delay is neglected, which is equivalence to that the oscillatory-type response function radiates for an infinity time. That is reason that MI gain approaches to infinity value.

This research was supported by the National Natural Science Foundation of China (Grant Nos. 11174090, 11174091, 11074080, and 11204299).

- [1] A. W. Snyder and D. J. Mitchell, *Science* **276**, 1538 (1997).
- [2] W. Królikowski, O. Bang, N. I. Nikolov, D. Neshev, J. Wyller, J. J. Rasmussen, and D. Edmundson, "Modulational instability, solitons and beam propagation in spatially nonlocal nonlinear media," *J. Opt. B: Quantum Semiclass. Opt.* **6**, S288 (2004).
- [3] M. Mitchell, M. Segev, and D. N. Christodoulides, "Observation of Multihump Multimode Solitons," *Phys. Rev. Lett.* **80**, 4657 (1998).
- [4] C. Conti, M. Peccianti, and G. Assanto, "Route to Nonlocality and Observation of Accessible Solitons," *Phys. Rev. Lett.* **91**, 073901 (2003);
- [5] C. Conti, M. Peccianti, and G. Assanto, "Observation of Optical Spatial Solitons in a Highly Nonlocal Medium," *Phys. Rev. Lett.* **92**, 113902 (2004).
- [6] M. Peccianti, C. Conti, G. Assanto, A. De Luca and C. Umeton, "Routing of nisolropic spatial solitons and modulational instability in liquid crystals," *Nature* **432**, 733 (2004).
- [7] W. Hu, T. Zhang, Q. Guo, L. Xuan, and S. Lan, "Nonlocality-controlled interaction of spatial solitons in nematic liquid crystals," *Appl. Phys. Lett.* **89**, 071111 (2006).
- [8] C. Rotschild, O. Cohen, O. Manela, M. Segev, and T. Carmon, "Solitons in Nonlinear Media with an Infinite Range of Nonlocality: First Observation of Coherent Elliptic Solitons and of Vortex-Ring Solitons," *Phys. Rev. Lett.* **95**, 213904 (2005).
- [9] B. Alfassi, C. Rotschild, O. Manela, M. Segev, and D. N. Christodoulides, "Nonlocal Surface-Wave Solitons," *Phys. Rev. Lett.* **98**, 213901 (2007).
- [10] A. Dreischuh, D. N. Neshev, D. E. Petersen, O. Bang, and W. Krolikowski, "Observation of Attraction between Dark Solitons," *Phys. Rev. Lett.* **96**, 043901 (2006).
- [11] C. Conti, A. Fratalocchi, M. Peccianti, G. Ruocco, and S. Trillo, "Observation of a Gradient Catastrophe Generating Solitons," *Phys. Rev. Lett.* **102**, 083902 (2009).
- [12] C. R. Rosberg, F. H. Bennet, D. N. Neshev, P. D. Rasmussen, O. Bang, W. Krolikowski, A. Bjarklev, and Y. S. Kivshar, "Tunable diffraction and self-defocusing in liquid-filled photonic crystal fibers," *Opt. Express* **15**, 12145 (2007).
- [13] P. D. Rasmussen, F. H. Bennet, D. N. Neshev, A. A. Sukhorukov, C. R. Rosberg, W. Krolikowski, O. Bang, and Y. S. Kivshar, "Observation of two-dimensional nonlocal gap solitons," *Opt. Lett.* **34**, 295 (2009).
- [14] S. Skupin, M. Saffman, and W. Królikowski, "Nonlocal Stabilization of Nonlinear Beams in a Self-Focusing Atomic Vapor," *Phys. Rev. Lett.* **98**, 263902 (2007).
- [15] P. Pedri and L. Santos, "Two-Dimensional Bright Solitons in Dipolar Bose-Einstein Condensates," *Phys. Rev. Lett.* **95**, 200404 (2005).
- [16] I. Tikhonenkov, B. A. Malomed, and A. Vardi, "Anisotropic Solitons in Dipolar Bose-Einstein Condensates," *Phys. Rev. Lett.* **100**, 090406 (2008).
- [17] D. Briedis, D. E. Petersen, D. Edmundson, W. Krolikowski, and O. Bang, "Ring vortex solitons in nonlocal nonlinear media," *Opt. Express* **13**, 435 (2005).
- [18] Y. V. Kartashov, V. A. Vysloukh, and L. Torner, "Stability of vortex solitons in thermal nonlinear media with cylindrical symmetry," *Opt. Express* **15**, 9378 (2007).
- [19] C. Rotschild, M. Segev, Z. Y. Xu, Y. V. Kartashov, L. Torner, and O. Cohen, "Two-dimensional multipole solitons in nonlocal nonlinear media," *Opt. Lett.* **31**, 3312-3314 (2006).
- [20] Z. Y. Xu, Y. V. Kartashov, and L. Torner, "Upper threshold for stability of multipole-mode solitons in nonlocal nonlinear media," *Opt. Lett.* **30**, 3171-3173 (2005).
- [21] D. Buccoliero, A. S. Desyatnikov, W. Krolikowski, and Y. S. Kivshar, "Laguerre and Hermite Soliton Clusters in Nonlocal Nonlinear Media," *Phys. Rev. Lett.* **98**, 053901 (2007).
- [22] D. Deng, and Q. Guo, "Ince-Gaussian solitons in strongly nonlocal nonlinear media," *Opt. Lett.* **32**, 3206 (2007).
- [23] D. Deng, X. Zhao, Q. Guo, and S. Lan, "Hermite-Gaussian breathers and solitons in strongly nonlocal nonlinear media," *J. Opt. Soc. Am. B* **24**, 2537 (2007).
- [24] Y. V. Izdebskaya, A. S. Desyatnikov, and Y. S. Kivshar, "Self-Induced Mode Transformation in Nonlocal Nonlinear Media," *Phys. Rev. Lett.* **111**, 123902 (2013).
- [25] Q. Shou, X. Zhang, W. Hu, and Q. Guo, "Large phase shift of spatial solitons in lead glass," *Opt. Lett.* **36**, 4194 (2011).

- [26] D. Q. Lu, W. Hu, Y. J. Zheng, Y. B. Liang, L. G. Cao, S. Lan, and Q. Guo, “Self-induced fractional Fourier transform and revivable higher-order spatial solitons in strongly nonlocal nonlinear media,” *Phys. Rev. A* **78**, 043815 (2008).
- [27] O. Bang, W. Królikowski, J. Wyller, and J. J. Rasmussen, “Collapse arrest and soliton stabilization in non-local nonlinear media,” *Phys. Rev. E* **66**, 046619 (2002).
- [28] Q. Shou, Y. B. Liang, Q. Jiang, Y. J. Zheng, S. Lan, W. Hu, and Q. Guo, *Opt. Lett.* **34**, 3523 (2009).
- [29] N. Ghofraniha, C. Conti, G. Ruocco, and S. Trillo, *Phys. Rev. Lett.* **99**, 043903 (2007).
- [30] X. Gao, J. Wang, L. Zhou, Z. Yang, X. Ma, D. Lu, Q. Guo, and W. Hu, *Opt. Lett.* **39**, 3760 (2014).
- [31] N. I. Nikolov, D. Neshev, O. Bang, and W. Królikowski, *Phys. Rev. E* **68**, 036614 (2003).
- [32] M. Bache, O. Bang, J. Moses, and F. W. Wise, *Opt. Lett.* **32**, 2490 (2007).
- [33] M. Bache, O. Bang, W. Królikowski, J. Moses, and F. W. Wise, *Opt. Express* **16**, 3273 (2008).
- [34] P. V. Larsen, M. P. Sørensen, O. Bang, W. Królikowski, and S. Trillo, *Phys. Rev. E* **73**, 036614 (2006).
- [35] J. Wyller, W. Królikowski, O. Bang, D. E. Petersen, and J. J. Rasmussen, *Phys. D* **227**, 8 (2007).
- [36] A. V. Buryak and Yu. S. Kivshar, *Phys. Lett. A* **197**, 407 (1995).
- [37] B. K. Esbensen, M. Bache, W. Królikowski, and O. Bang, *Phys. Rev. A* **86**, 023849 (2012).
- [38] J. Wang, Y. Li, Q. Guo, and W. Hu, *Opt. Lett.* **39**, 405 (2014).
- [39] M. Peccianti and G. Assanto, *Phys. Rep.* **516**, 147 (2012).
- [40] E. Braun, L. P. Faucheux, and A. Libchaber, *Phys. Rev. A* **48**, 611 (1993).
- [41] M. Warenghem, J. F. Henninot, and G. Abbate, *Opt. Express* **2**, 438 (1998).
- [42] M. A. Karpierz, M. Sierakowski, M. Swillo, and T. Wolinsky, *Mol. Cryst. Liq. Cryst.* **320**, 157 (1998).
- [43] M. Peccianti, G. Assanto, A. De Luca, C. Umeton, and I. C. Khoo, *Appl. Phys. Lett.* **77**, 7 (2000).
- [44] M. Peccianti, K. A. Brzdakiewicz, and G. Assanto, *Opt. Lett.* **27**, 1460 (2002).
- [45] W. Hu, S. Ouyang, P. Yang, Q. Guo, and S. Lan, *Phys. Rev. A* **77**, 033842 (2008).
- [46] B. D. Skuse, and N. L. Smyth, *Phys. Rev. A* **77**, 013817 (2008).
- [47] A. Piccardi, A. Alberucci, N. Tabiryan, and G. Assanto, *Opt. Lett.* **36**, 1356 (2011).
- [48] M. F. Schiekel and K. Fahrenschon, *Appl. Phys. Lett.* **19**, 391 (1971).
- [49] L. Z. Ruan, Fuzi Yang, and J. R. Sambles, *Appl. Phys. Lett.* **93**, 031909 (2008).